Electronic structure of the Ba_4C_{60} superconductor

Koichiro Umemoto and Susumu Saito
Department of Physics, Tokyo Institute of Technology, 2-12-1 Oh-okayama, Meguro-ku, Tokyo 152-8551, Japan
(Received 18 January 2000)

We study the electronic structure of the superconducting body-centered-orthorhombic fulleride Ba_4C_{60} using the local-density approximation in the density-functional theory. It is found that Ba states are strongly hybridized with C_{60} states through pentagons, explaining the observed lattice-constant differences, $a>b>c$. Due to this hybridization and to a rather low symmetry of the lattice causing the splitting of states, the t_{1g}-derived conduction band partially occupied by two electrons is found to be relatively wide. Fermi surfaces also show noncubic nature and contain dual quasiplanar sheets parallel to the a-b plane in the momentum space, giving rise to a quasinesting vector parallel to the c axis.

I. INTRODUCTION

Face-centered-cubic (fcc) alkali fullerides, A_3C_{60} with A = K, Rb, or the combinations of Na, K, Rb, and Cs, have been intensively studied due to their high superconducting transition temperatures (T_c) observed.[1–7] In A_3C_{60}, alkali atoms donate their valence electrons to the otherwise empty conduction band derived from the lowest-unoccupied t_{1u} state of the C_{60} cluster, giving rise to a half-filled conduction band.[8–10] The variation of their T_c is believed to be mostly governed by the value of the Fermi-level density of states $[N(E_F)]$, which is one of the most important parameters in the BCS-type theory of superconductivity.[11–13]

In addition to A_3C_{60}, several alkaline-earth fullerides have been also synthesized and some of them are reported to be metallic and even superconducting. In the case of Ba and Sr fullerides, a recent work has clarified that Ba_4C_{60} and Sr_4C_{60} with the body-centered-orthorhombic (bco) cell are the superconducting phase.[14] They are the first noncubic C_{60} superconductors among alkali and alkaline-earth fullerides at ambient pressure reported so far. Also they are the first C_{60} superconductors free from any geometrical disorder; A_3C_{60} superconductors other than Na_2RbC_{60} and Na_2CsC_{60} are known to possess so-called merohedral disorder of C_{60} orientations, while Na_2RbC_{60} and Na_2CsC_{60} possess the glass orientational disorder of C_{60} at lower temperatures[15,16] as in the case of the pristine solid C_{60}.[17,18] Also the bcc $K_3Ba_3C_{60}$ superconductor is known to have a random occupancy of K and Ba ions.[19,20] Therefore, the electronic structure of disorder-free Ba_4C_{60} and Sr_4C_{60} is of high interest because they can deserve a detailed comparison between theory and experiment in the future. Since there are eight valence electrons per unit cell, the t_{1u} band may be fully filled and the next t_{1g} band may be partially occupied by only two electrons, being well below the half-filling of the t_{1g} band. They are also interesting opposites of Cs_4C_{60} that are reported to have very similar geometry[21] but should have two holes in the t_{1u} band. In sharp contrast to superconducting Ba_4C_{60} and Sr_4C_{60}, A_4C_{60} including Cs_4C_{60} are reported to be nonmetallic.[22–27]

In the present paper, we study the electronic structure of Ba_4C_{60}, of which the full geometry has been already reported experimentally,[14] using the local-density approximation (LDA) within the framework of the density-functional theory.[28] We find that Ba states are strongly hybridized with C_{60} states via pentagons, which stabilizes the low-symmetry bco lattice. The hybridization-caused low symmetry is found to play a key role in the peculiar behaviors of the electronic states in superconducting Ba_4C_{60}.

II. COMPUTATIONAL METHOD

In the electronic-structure calculations, we adopt the Ceperley-Alder exchange-correlation potential[29] in the LDA. The norm-conserving pseudopotentials[30] with the Kleinman-Bylander separable approximation[31] are also adopted. The real-space-partition method[32] is used in order to avoid the breakdown of the separable approximation for Ba. A plane-wave basis set with a cutoff energy of 50 Ry is used. In the Ba atom, it is known that there is a considerable spatial overlap between valence states and the highest-energy core p states ($5p$ states).[33] Therefore, we treat Ba $5p$ states as not core states but valence states in order to include this effect. The structure of Ba_4C_{60} to be studied is schematically shown in Fig. 1. There are three different lattice constants [a = 11.6101 Å, b = 11.2349 Å, c = 10.8830 Å (Ref. 14)] and two different Ba sites because of its orthorhombic geom-

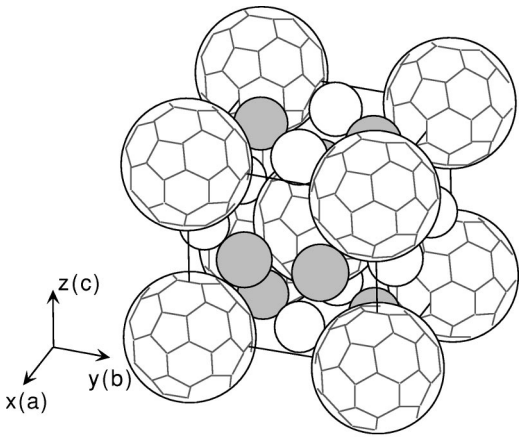

FIG. 1. Structure of Ba_4C_{60} studied in the present work. Shaded and white spheres denote Ba(1) and Ba(2) atoms, respectively.

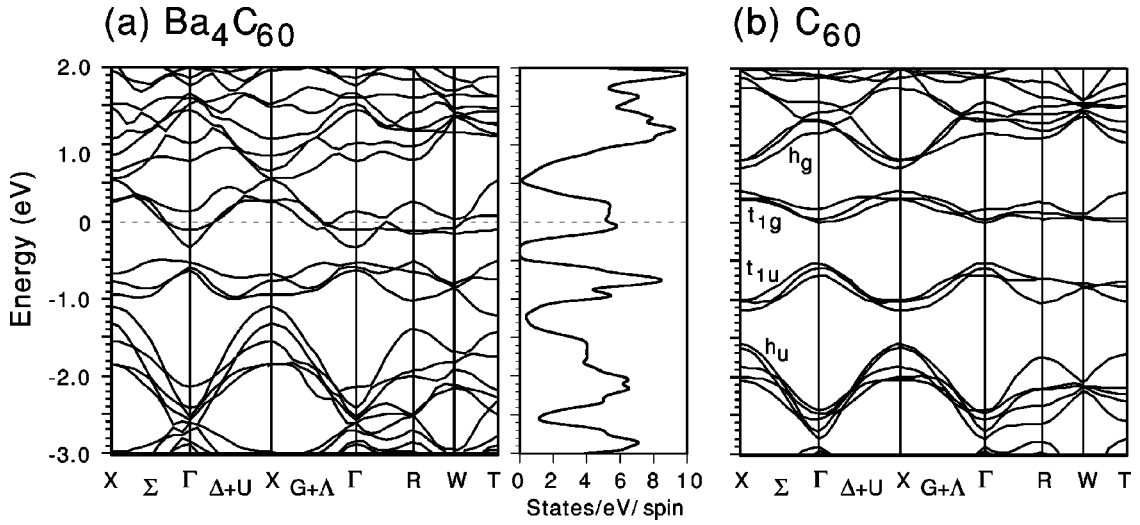

FIG. 2. (a) The band structure (square panel) and the density of states (rectangular panel) of Ba_4C_{60} and (b) the band structure of the hypothetical pristine C_{60}. Since a, b, and c axes are different from one another in the orthorhombic structure, there are three distinct lines from Γ point to X point, i.e., Σ, $\Delta+U$, and $\Lambda+G$ lines along k_x, k_y, and k_z axes in the momentum space, respectively. In (a), energy is measured from the Fermi level denoted by the horizontal broken line. The density of states is broadened by using the Gaussian-distribution function with the width of 0.001 eV. In (b), energy scale is the same as that in (a). U and G lines are on a small rectangular facet of the Brillouin zone and are very short in this fulleride [cf. Fig. 4(d)].

etry, which does not have threefold symmetry axes. As for geometries and lattice constants, we use experimental values with the same Ba(1) and (2) notations.[14] In addition to Ba_4C_{60}, we also study a hypothetical pristine C_{60} in order to perform a comparative study between Ba_4C_{60} and the pristine bco C_{60}. Lattice constants and coordinates of the hypothetical pristine bco C_{60} are assumed to be identical to those of Ba_4C_{60}.

III. RESULTS AND DISCUSSION

The band structure and density of states (DOS) of Ba_4C_{60} obtained are shown in Fig. 2(a) and the band structure of the hypothetical pristine bco C_{60} in Fig. 2(b). The widths of t_{1g}-derived band in the pristine C_{60} and Ba_4C_{60}, which are represented by the difference between the highest eigenvalue among three t_{1g} states at the X point and the lowest at the Γ point, are 0.40 eV and 0.88 eV, respectively. This widening

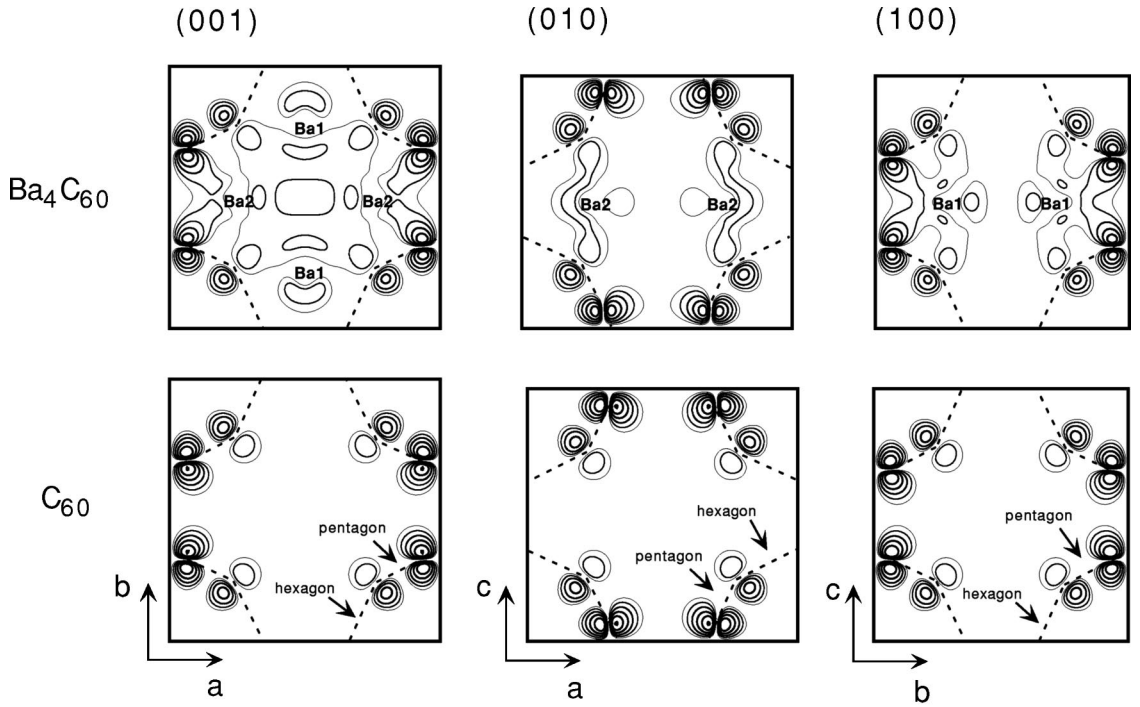

FIG. 3. Spatial distributions of the t_{1g} states in Ba_4C_{60} (upper panels) and in the bco pristine C_{60} (lower panels). Each contour line indicates twice (half) the density of the neighboring thinner (thicker) contour lines. The minimum density denoted by the thinnest line in this figure is 6.25×10^{-4} a.u.$^{-3}$. ''Ba1'' and ''Ba2'' represent positions of Ba(1) and Ba(2) atoms, respectively.

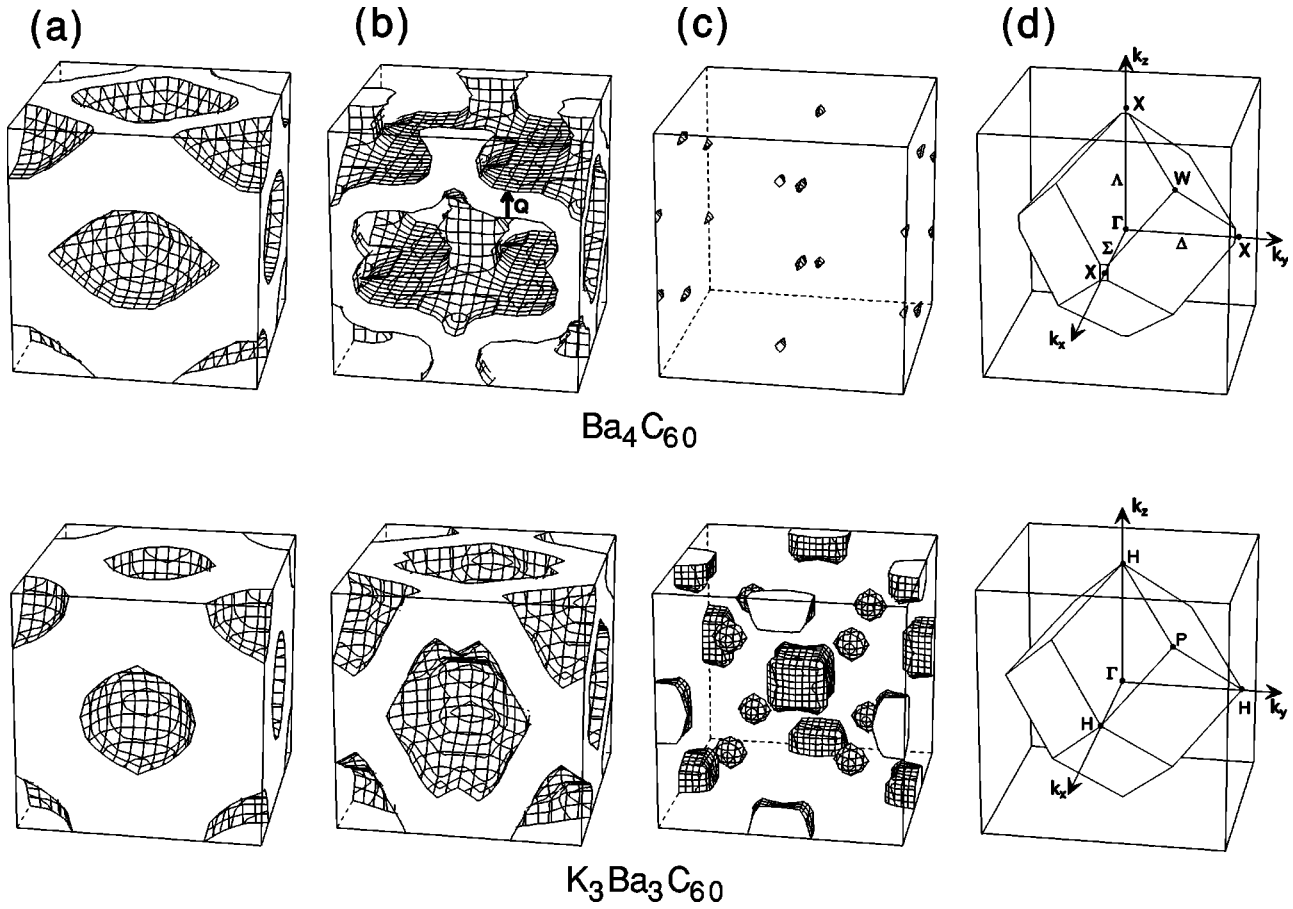

FIG. 4. Fermi surfaces on (a) the lowest, (b) the middle, and (c) the highest state of the t_{1g} band, in Ba_4C_{60} (upper panels) and $K_3Ba_3C_{60}$ (lower panels). In each figure, the region shown is wider than the first Brillouin zone that is shown in (d) with the names of selected symmetry points and lines. All the surfaces have electrons inside. In (b) of Ba_4C_{60}, **Q** represents the quasinesting vector.

of the t_{1g} band upon the inclusion of Ba indicates the presence of the hybridization between C_{60}-t_{1g} and Ba states in Ba_4C_{60} as has been observed in other bcc Ba fullerides.[34–37] For the sake of simplicity, we call the hybridized band of t_{1g} and Ba states hereafter the ''t_{1g} band.'' Owing to its lower symmetry, the degeneracy appearing in cubic fullerides at symmetry points is considerably lifted in bco Ba_4C_{60}. Even in the pristine bco C_{60}, the difference between the top and bottom states of the t_{1g} band at the Γ point is as large as 0.16 eV. In Ba_4C_{60}, the presence of four Ba atoms is found to give a more prominent band dispersion and to lift the degeneracy even more. Consequently, the uppermost branch of the t_{1g} band is almost empty and does not cross the Fermi level except along the Λ line. The difference between the top and bottom states of the t_{1g} band at the Γ point in Ba_4C_{60} is now 0.46 eV, being much larger than that of the pristine bco C_{60}. It is also caused by the lifting of the degeneracy due to the low symmetry that the t_{1g} bandwidth of Ba_4C_{60} is as wide as that of bcc Ba_6C_{60}.[34–36]

The Fermi level lies in the t_{1g} band that is occupied by two electrons, as expected stoichiometrically. The DOS value at Fermi level $N(E_F)$ is 5.3 states/eV spin, which is in good accord with the experimental value of 6.0 states/eV spin.[14] This calculated $N(E_F)$ of Ba_4C_{60} is larger than that of Ba_6C_{60} (4.3 states/eV spin),[36] being consistent with the superconductivity observed not in Ba_6C_{60} but in Ba_4C_{60}. Interestingly, the gap between t_{1g} and next h_g bands, which is directly at the X point, is found to be almost negligible, 0.013 eV. Therefore, the conduction band is not an energetically isolated narrow band unlike fcc A_3C_{60}.

Figure 3 shows spatial distributions of t_{1g} states $\rho_{t_{1g}}$,

$$\rho_{t_{1g}}(\mathbf{r}) = \sum_n \int d\mathbf{k} \int dE |\Psi_{n\mathbf{k}}|^2 \delta(E - \epsilon_{n\mathbf{k}}),$$

in Ba_4C_{60} and the hypothetical pristine bco C_{60}. Here, the energy integration is done in the energy range covering whole three branches of the t_{1g} band, and the same sampling points as used in the self-consistent electronic-structure calculation are taken for the **k** integration. These figures indicate that both Ba(1) and Ba(2) ''pull'' t_{1g} states, which are originally distributed mostly above pentagons in the pristine bco C_{60}, and that t_{1g} states are hybridized with Ba states through pentagons. As can be clearly seen from the figure on

TABLE I. Observed T_c and $N(E_F)$ and the calculated $N(E_F)$ of Ba_4C_{60} and $K_3Ba_3C_{60}$. The unit of $N(E_F)$ is states/eV spin. Experimental data for Ba_4C_{60} and $K_3Ba_3C_{60}$ are from Ref. 14 and Ref. 20, respectively.

	T_c (K)	$N(E_F)$ (expt.)	$N(E_F)$ (theory)
Ba_4C_{60}	6.7	6.0	5.3
$K_3Ba_3C_{60}$	5.6	5.7	5.7

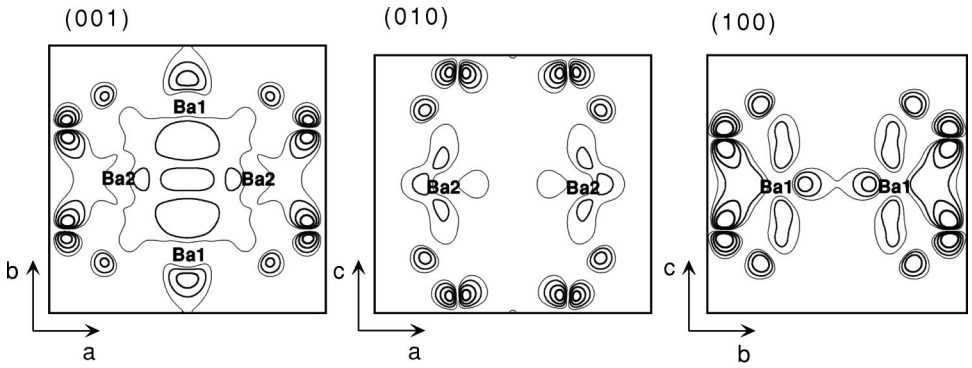

FIG. 5. Spatial distributions of states near the Fermi level in Ba_4C_{60}. Each contour line indicates twice (half) the density of the neighboring thinner (thicker) contour lines. The minimum density denoted by the thinnest line in this figure is 3.125×10^{-4} a.u.$^{-3}$.

the (001) plane, the hybridization, which should give rise to an attractive interaction, along the b axis between t_{1g} and Ba(2) states, is definitely stronger than that along the a axis with Ba(1) states, being consistent with the observed lattice-constant difference $a>b$. On the other hand, the shortest c value can be explained by the existence of unoccupied interstitial sites along the c axis and a strong hybridization between t_{1g} and Ba(1) states on the (100) plane.

Figure 4 shows the Fermi surfaces of Ba_4C_{60} originating from three branches of the t_{1g} band. In order to perform a comparative study between noncubic Ba_4C_{60} and cubic $K_3Ba_3C_{60}$ superconductors, the Fermi surfaces of $K_3Ba_3C_{60}$ are also shown in Fig. 4. Theoretical methods used in the electronic-structure calculation for $K_3Ba_3C_{60}$ are common to those for Ba_4C_{60} and have been explained in Ref. 37. In these two fullerides, T_c and $N(E_F)$ are rather close to each other (Table I). In Ba_4C_{60}, there are closed hole orbits around X points on the Fermi surfaces originating from the lowest t_{1g} state. The Fermi surface from the next state, which has the largest contribution to $N(E_F)$ (64%), clearly shows noncubic nature of the bco lattice and consists of dual quasiplanar sheets normal to the k_z axis, which are connected to each other by a cylinder along the Λ line. These quasiplanar sheets give rise to open orbits normal to the k_z axis and at the same time a nesting nature of the Fermi surfaces with the nesting vector $\boldsymbol{Q}=\pm Q\boldsymbol{k}_z$ with $Q\simeq0.2(2\pi/c)$ is shown in Fig. 4(b). Thus, the attractive electron-electron interaction mediated by phonons of the wave vector $\boldsymbol{Q}$ should become strong. Fermi surfaces originating from the highest t_{1g} state are very small; therefore they should contribute little to electronic transport properties. In $K_3Ba_3C_{60}$, Fermi surfaces from the lowest t_{1g} state are similar to those of Ba_4C_{60} and there are closed hole orbits around H points. Interestingly, the next state possesses a little larger hole surfaces also around H points, reflecting the similar dispersion characters of the lower two branches of the t_{1g} band in $K_3Ba_3C_{60}$.[37] Since $K_3Ba_3C_{60}$ has a half-filled t_{1g} band with one more electron than Ba_4C_{60}, the highest t_{1g} state has fairly wide Fermi surfaces, i.e., closed electron orbits around Γ and P points.

In Fig. 5, spatial distributions of the states near the Fermi level ρ_{E_F},

$$\rho_{E_F}(\mathbf{r})=\sum_n \int d\mathbf{k}\int_{E_F-\Delta}^{E_F+\Delta} dE|\Psi_{n\mathbf{k}}|^2\delta(E-\epsilon_{n\mathbf{k}}),$$

on each plane in Ba_4C_{60} are shown. Here $\Delta=0.1$ eV, which is the typical phonon energy in fullerides, is used. Figure 5 indicates that superconducting carriers should be on C_{60} clusters, around Ba sites, in the interfullerene area on the (001) plane, and in the area between two Ba(1) atoms. Therefore, the carriers may be coupled not only with C_{60} intrafullerene phonons but also with the optical phonons involving Ba-ion displacements. The isotope effect of Ba as well as that of C atoms may be present. Interestingly, ρ_{E_F} in Ba_4C_{60} seems to spread more uniformly than that in Ba_6C_{60}.[35] This may give a weaker Coulomb repulsion between carriers in Ba_4C_{60}, being again consistent with the superconductivity reported not in Ba_6C_{60} but in Ba_4C_{60}.

IV. SUMMARY

We have studied the electronic structure of the superconducting bco Ba_4C_{60} by using the local-density approximation within the framework of the density-functional theory. It has been found that Ba states are hybridized with C_{60}-t_{1g} states through pentagons. The t_{1g} bandwidth of Ba_4C_{60}, occupied partially by two electrons, has been found to be as wide as that of Ba_6C_{60} due to the hybridization and the low symmetry that lifts the degeneracies of the electronic states even at symmetry points. The hybridization between t_{1g} and Ba states naturally explains a relationship among lattice constants $a>b>c$. Fermi surfaces are found to contain dual quasiplanar sheets parallel to the ab plane with a quasinesting vector parallel to the c axis. Because carriers to be responsible for superconductivity have been found to be not only on C_{60} clusters but also around Ba sites, the hybridization between C_{60} and Ba states should play an important role in superconductivity.

ACKNOWLEDGMENTS

We would like to thank Professor Y. Iwasa and coworkers for providing their work prior to publication. This work was supported by a Grant-in-Aid for Scientific Research on the Priority Area ''Fullerenes and Nanotubes'' by the Ministry of Education, Science, and Culture of Japan, the Nissan Science Foundation, and the Japan Society for the Promotion of Science (Project No. 96P00203). We have used programs for electronic-structure calculations by A. Oshiyama, T. Nakayama, M. Saito, O. Sugino, and N. Hamada. Numerical calculations were performed on Fujitsu VPP500 at the Institute for Solid State Physics, University of Tokyo, and NEC SX3/R at Institute for Molecular Science, Okazaki National Institute.

[1] A.F. Hebard, M.J. Rosseinsky, R.C. Haddon, D.W. Murphy, S.H. Glarum, T.T.M. Palstra, A.P. Ramirez, and A.R. Kortan, Nature (London) **350**, 600 (1991).
[2] P.W. Stephens, L. Mihaly, P.L. Lee, R.L. Whetten, S.M. Huang, R. Kaner, F. Deiderich, and K. Holczer, Nature (London) **351**, 632 (1991).
[3] M.J. Rosseinsky, A.P. Ramirez, S.H. Glarum, D.W. Murphy, R.C. Haddon, A.F. Hebard, T.T.M. Palstra, A.R. Kortan, S.M. Zahurak, and A.V. Makhija, Phys. Rev. Lett. **66**, 2830 (1991).
[4] K. Tanigaki, T.W. Ebbesen, S. Saito, J. Mizuki, J.S. Tsai, Y. Kubo, and S. Kuroshima, Nature (London) **352**, 222 (1991).
[5] K. Holczer, O. Klein, S.M. Huang, R.B. Kaner, K.J. Fu, R.L. Whetten, and F. Diederich, Science **252**, 1154 (1991).
[6] G. Sparn, J.D. Thompson, R.L. Whetten, S.M. Huang, R.B. Kaner, F. Diederich, G. Grüner, and K. Holczer, Phys. Rev. Lett. **68**, 1228 (1992).
[7] K. Tanigaki, I. Hirosawa, T.W. Ebbesen, J. Mizuki, and J.S. Tsai, J. Phys. Chem. Solids **54**, 1645 (1993).
[8] S. Saito and A. Oshiyama, Phys. Rev. B **44**, 11 536 (1991).
[9] S.C. Erwin and W.E. Pickett, Science **254**, 842 (1991).
[10] J.L. Martins and N. Troullier, Phys. Rev. B **46**, 1766 (1992).
[11] C.M. Varma, J. Zaanen, and K. Raghavachari, Science **254**, 989 (1991).
[12] A. Oshiyama and S. Saito, Solid State Commun. **82**, 41 (1992).
[13] M. Schluter, M. Lannoo, M. Needels, G.A. Baraff, and D. Tománek, Phys. Rev. Lett. **68**, 526 (1992).
[14] C.M. Brown, S. Taga, B. Gogia, K. Kordatos, S. Margadonna, K. Prassides, Y. Iwasa, K. Tanigaki, A.N. Fitch, and P. Pattison, Phys. Rev. Lett. **83**, 2258 (1999).
[15] K. Kniaz, J.E. Fischer, Q. Zhu, M.J. Rosseinsky, O. Zhou, and D.W. Murphy, Solid State Commun. **88**, 47 (1993).
[16] K. Prassides, C. Christides, I.M. Thomas, J. Mizuki, K. Tanigaki, I. Hirosawa, and T.W. Ebbesen, Science **263**, 950 (1994).
[17] W.I.F. David, R.M. Ibberson, J.C. Metthewman, K. Prassides, T.J.S. Dennis, J.P. Hare, H.W. Kroto, R. Taylor, and D.R.M. Walton, Nature (London) **353**, 147 (1991).
[18] W.I.F. David, R.M. Ibberson, T.J.S. Dennis, J.P. Hare, and K. Prassides, Europhys. Lett. **18**, 219 (1992).
[19] Y. Iwasa, H. Hayashi, T. Furudate, and T. Mitani, Phys. Rev. B **54**, 14 960 (1996).
[20] Y. Iwasa, M. Kawaguchi, H. Iwasaki, T. Mitani, N. Wada, and T. Hasegawa, Phys. Rev. B **57**, 13 395 (1998).
[21] P. Dahlke, P.F. Henry, and M.J. Rosseinsky, J. Mater. Chem. **8**, 1571 (1998).
[22] R.M. Fleming, M.J. Rosseinsky, A.P. Ramirez, D.W. Murphy, J.C. Tully, R.C. Haddon, T. Siegrist, R. Tycko, S.H. Glarum, P. Marsh, G. Dabbagh, S.M. Zahurak, A.V. Makhija, and C. Hampton, Nature (London) **352**, 701 (1991).
[23] M. Kosaka, K. Tanigaki, I. Hirosawa, Y. Shimakawa, S. Kuroshima, T.W. Ebbesen, J. Mizuki, and Y. Kubo, Chem. Phys. Lett. **203**, 429 (1993).
[24] F. Stepniak, P.J. Benning, D.M. Poirier, and J.H. Weaver, Phys. Rev. B **48**, 1899 (1993).
[25] S.C. Erwin and C. Bruder, Physica B **199&200**, 600 (1994).
[26] C.A. Kuntscher, G.M. Bendele, and P.W. Stephens, Phys. Rev. B **55**, R3366 (1997).
[27] M. Knupfer and J. Fink, Phys. Rev. Lett. **79**, 2714 (1997).
[28] P. Hohenberg and W. Kohn, Phys. Rev. **136**, B864 (1964); W. Kohn and L.J. Sham, *ibid.* **140**, A1133 (1965).
[29] J.P. Perdew and A. Zunger, Phys. Rev. B **23**, 5048 (1981); D.M. Ceperley and B.J. Alder, Phys. Rev. Lett. **45**, 566 (1980).
[30] N. Troullier and J.L. Martins, Phys. Rev. B **43**, 1993 (1990).
[31] L. Kleinman and D.M. Bylander, Phys. Rev. Lett. **48**, 1425 (1982).
[32] M. Saito, O. Sugino, and A. Oshiyama, Phys. Rev. B **46**, 2606 (1992).
[33] T. Charpentier, G. Zerah, and N. Vast, Phys. Rev. B **54**, 1427 (1996).
[34] S.C. Erwin and M.R. Pederson, Phys. Rev. B **47**, 14 657 (1993).
[35] S. Saito and A. Oshiyama, Phys. Rev. Lett. **71**, 121 (1993).
[36] S. Saito and A. Oshiyama, J. Phys. Chem. Solids **54**, 1759 (1993).
[37] K. Umemoto, S. Saito, and A. Oshiyama, Phys. Rev. B **60**, 16 186 (1999).